IOP Conf. Series: Journal of Physics: Conf. Series **1269** (2019) 012012 doi:10.1088/1742-6596/1269/1/012012

The mesospheric sodium layer and its impact on the LGS parameters

F. DJAIDRI[1,2], N. MOUSSAOUI[1]

[1]Faculté de Physique, Université des Sciences et de la Technologie Houari Boumediene, BP32 El- Alia, Bab- Ezzouar, Algiers, Algeria
[2]Faculté des Sciences, Université M'Hamed Bouguerra, Avenue de l'Indépendance 35000, Boumerdès, Algeria

fdjaidri@usthb.dz

Abstract. The atmospheric turbulence limits the angular resolution of telescopes of tens of meters to that of a telescope of 20 cm diameter. Large telescopes, such as the VLT and the E-ELT, have adopted the Adaptive Optics (AO) system to reduce the undesirable effects of turbulence. The implantation of the technology of "sodium-LGSs" is essential to increase the performances of the AO. The generation of "sodium-LGSs" is the result of the fluorescence of mesospheric Na atoms located between 80 to 105 km of altitude. The laser beam sent from the ground is tuned to the wavelength 589 nm; excites the D_2 line of Na. The backscattered light gives necessary information on atmospheric turbulence and their effects on the incoming wave front of an astronomical object. The mesospheric sodium layer is characterized by the abundance of Na, the centroid height and the thickness of the layer. Their behaviors affect the variations of parameters of the "sodium-LGSs", such as the Return Flux and the elongation of the spot. The characterization of this layer is necessary in order to optimize the performance of the "LGSs-AO" system. We present semi-empirical models based on experimental measurements. These models explain the variations in the abundance and height of the centroid of the sodium layer.

1. Introduction

It is known from Galileo that the quality of the optical images of the stars observed from the Earth is greatly degraded by the atmosphere. Technological and computational progress offer astronomy the new generation of large telescopes by combining the AO (use of deformable mirrors integrated in the telescope) and the laser-matter interaction by creating an artificial star (LGS) [1, 2]. Figure 1 represents the system of AO using LGS facility. This LGS should be in the field of view of the astronomical object. We can't talk about sodium-LGS without talking about the mesospheric sodium layer. This layer lies between 85-105 km altitudes. The sodium LGS allows to probe the effects of all atmospheric disturbing layers [3].

Today, astronomers look for ever farther and smaller objects using larger telescopes. The European project for the Extremely Large Telescope (E-ELT of 40 m in diameter), form part of this logic [2]. Current telescopes use LGSs, either single or multiple beacons. Figure 2, shows that E-ELT uses four LGSs-AO systems [4].

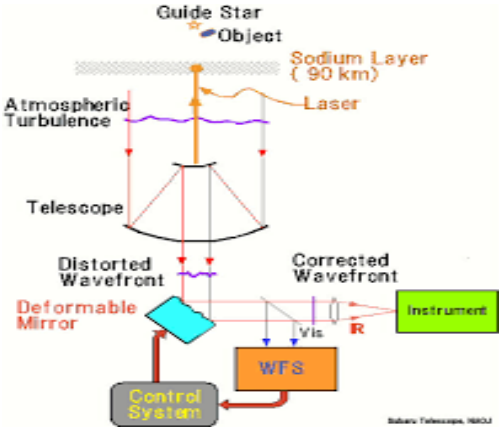

Figure 1. Configuration of AO's system [5].

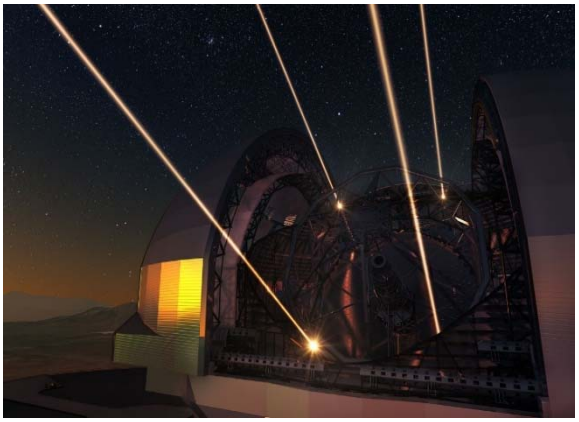

Figure 2. European Extremely Large Telescope's multi-LGSs system [6].

2. Different telescopes dimensions

The angular resolution allows us to distinguish the maximum of details of the objects observed. The new technology of the LGS- AO allows to increase the angular resolution of telescopes by just increasing their diameters.

It is given theoretically by the expression $1.22 \times \lambda / D$, where λ is the wavelength of the observed light and D is the diameter of the telescope. Figure 1 represents different telescopes in the world and compares their diameters [7].

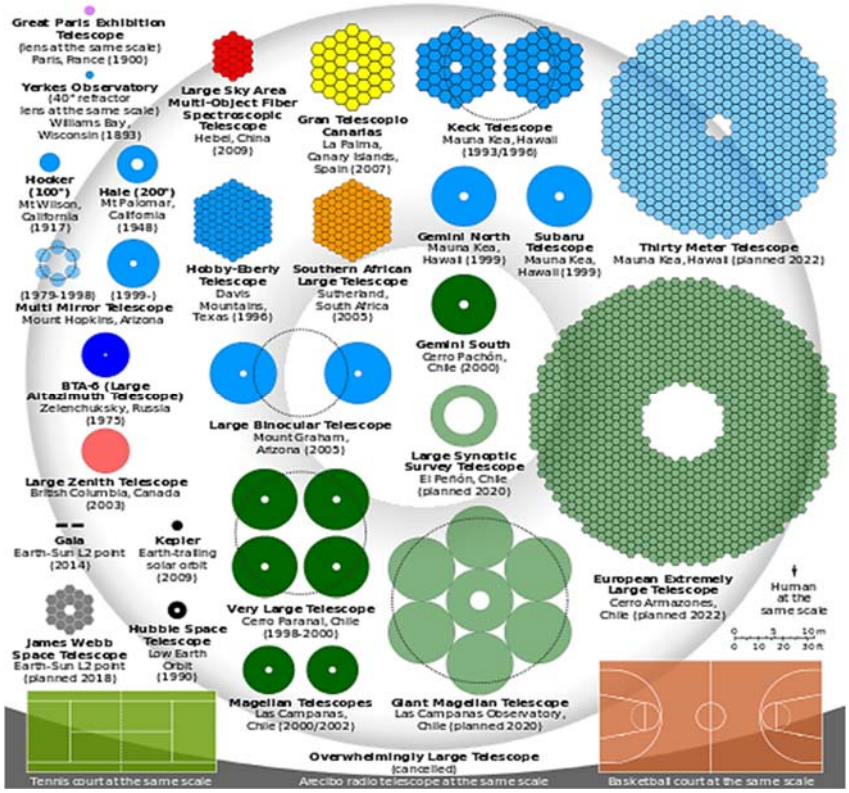

Figure 3. Comparison between primary mirrors of optical telescopes [8].

3. Results and discussion

3.1. Characteristics of the sodium layer

Sodium layer is characterized by three parameters: sodium abundance (C_{Na}), centroid height (H_{Na}), and thickness of layer (t_{Na}). Fig.4 represents an accumulation of two years experimental data. This figure shows a strong fluctuation during one year [2].

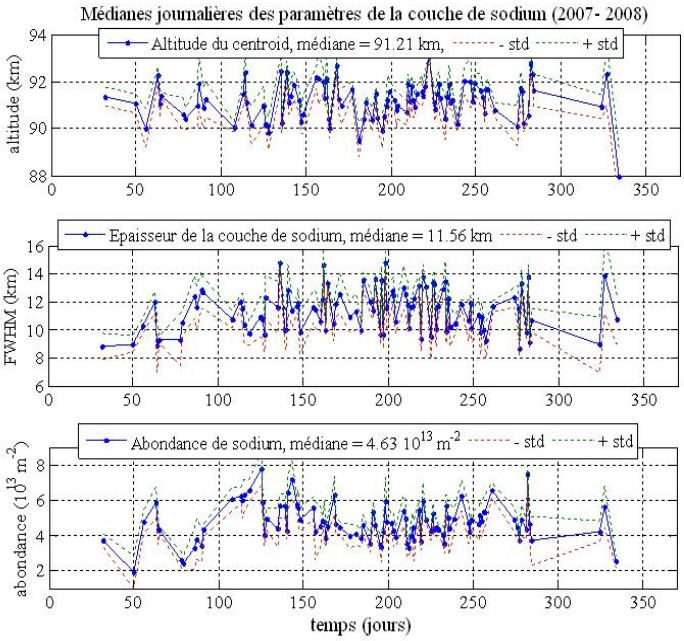

Figure 4. Daily median parameters of the sodium layer during one year.

3.1.1. Sodium layer abundance. In the next part, we present the abundance variation's model according to the results of Simonish, 1979. The Eq.1 represents the least mean squares fit of variation of column abundance C_{Na} (in 10^{13} m^{-2}) [9].

$$C_{Na}(t) = 4.38 - \cos(2\pi\frac{(t+6)}{365}) \times (1.16 + 0.27\cos(2\pi\frac{(t+77)}{4015})) + 0.61\cos(2\pi\frac{(t+77)}{4015}) \qquad (1)$$

Time (t) is in days. Using this equation, we obtain Figures 5 and 6.

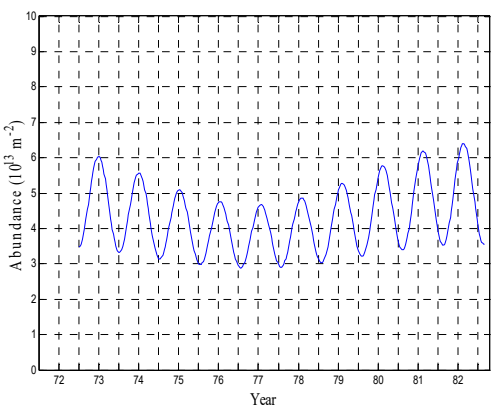

Figure 5. Column abundance variation for one solar cycle.

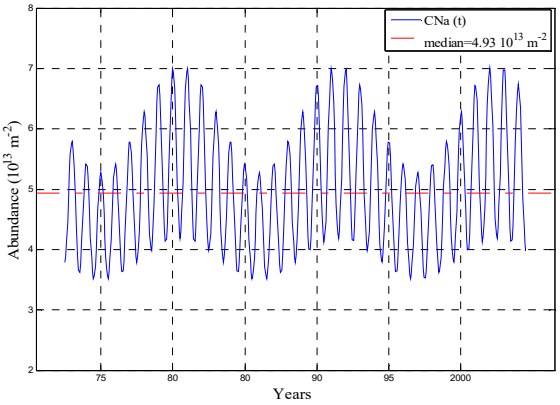

Figure 6. Column abundance, with (C_{Na0}= 5×10^{13} m^{-2}, the annual median value, in Moussaoui, 2010).

Both figures explain the variation of sodium abundance during a long time. Figure 5 represents the fitting of experimental data of Simonich, 1979 during one solar cycle.

3.1.2. Centroid sodium layer. The reference (Clemesha et al, 1997) represents the following relationship in (2). It expresses a least mean squares fit which shows the change in the centroid height $H_{Na}(t)$ depending of time, the period (1970-1995), represented in figure 8 [10].

$$H_{Na}(t) = H_0 + aT + bcos(\frac{2\pi T}{10} - T_0) \quad (2)$$

T is the time in years and T_0=1979.5, for the zero phase of the oscillation in peak centroid height. The linear tend a, is given by −37± 9 m yr^{-1} and b is the amplitude of the 10-yr cycle, given by 170± 110 m [10].

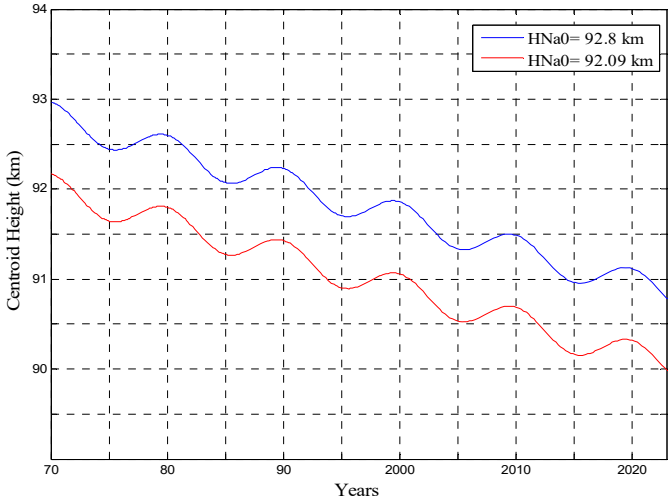

Figure 7. Centroid height for one Solar cycle

Figure 7 represents centroid height in long term, when it will possible to predict the variation as a function of solar cycles in future. Equation 2 can be applied up to the 24th solar cycle, when the centroid has a linear trend.

3.2. LGS's parameters

Our aim is to simulate the variations in parameters of E-ELT_LGSs. We know that return flux F_R is depending of the characteristics of the sodium layer. We have presented the return flux, using results of (1) and (2). Both abundance and centroid of mesospheric sodium layer vary as a function of time. We obtaine figure 8. The specific return photon to the ground flux (F_R) of sodium LGS is given by (3):

$$F_R(t) = \frac{s_{ce} C_{Na} T_{atmo}^{2sec(\xi)}}{H_{Na}^2 sec(\xi)} \quad (3)$$

T_{atmo}=0.89, is the coefficient transmission of the atmosphere at 589 nm at zenith, for single- pass. S_{ce} is the coupling efficiency of light at 589 nm to the atom of Na with (unit: photons x m^2/ s/ W/ atom). The sec (ξ) =1, is the secant of the zenith angle and H_{Na0}= 92.09 km according to [1].

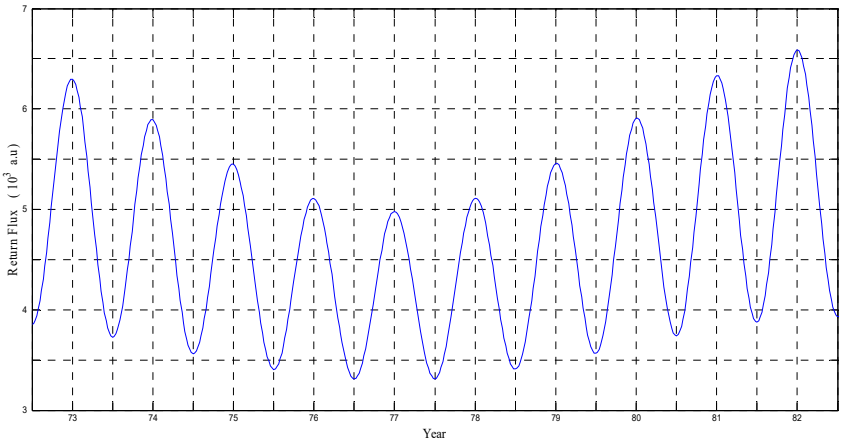

Figure 8. Variations of the Return Flux (F_R) for one solar cycle.

Figure 8 shows the variation of F_R, in arbitrary unit (au) duringone solar cycle. F_R is strongly dependent on the cycle, when the maximum appears at the beginning while the minimum appears in the middle of the solar cycle.

To find out which parameters affect the most F_R, we change each time a separate parameter. Figure 9 presents the centroid effect when changing H_0; the first term of (2). Figure 10 presents the variation of F_R for different experimental values of the transmission coefficient of T_{atmo}. Note that T_{atmo} depends on the sit.

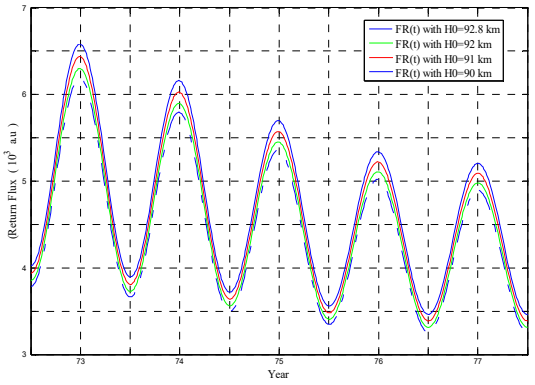

Figure 9. Variation of $F_R(t)$ as a fonction of $H_{Na}(t)$.

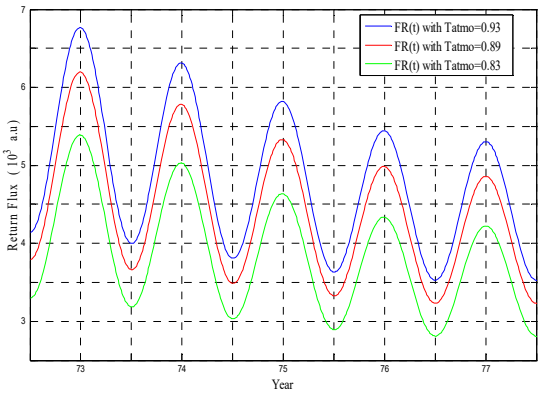

Figure 10. Variation of $F_R(t)$ on time in a half solar cycle with different values of T_{atmo}.

Figure 9 represents that the variation of 3 km of H_0 changes the flux by a single unit of value (1 au), while the variation of the atmospheric transmission coefficient of the different observation sites (T_{atmo} between 0.83 and 0.93) varies the flux by about 2 au, (see figure 10). We estimate that the variation of the centroid height has no influence on the variation of the return flux in a long term (see figure 9). Otherwise, F_R is affected quantitatively by T_{atmo}.

As the astronomical observation is made for a zenihal angle between 0 and 60 degrees, it remains therefore to vary the term of the secant in order to discuss its effect on F_R. Figure 11 represents the variation of F_R in function of time for different angles of observation.

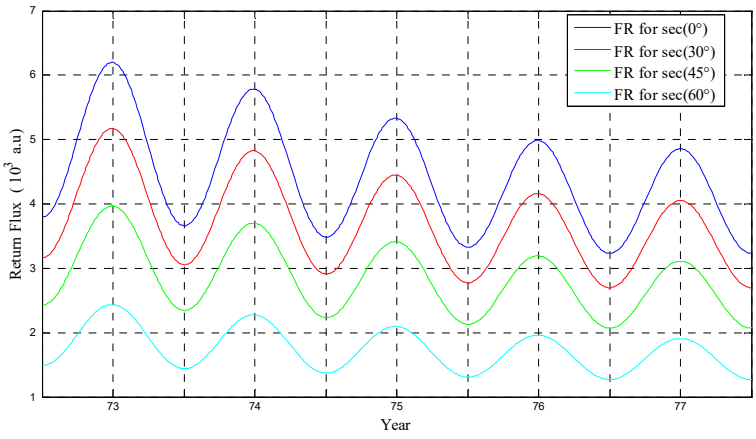

Figure 11. Variation of $F_R(t)$ as a fonction of observation's angle.

The term of secante represents the air mass parameter. Figure 11 shows that the F_R is strongly varied by varying the angle of observation with an attenuation about 60% at an angle of 60° comparing with F_R obtened at the zenith angle.

4. Conclusion

This study was done without taking into consideration the term S_{ce} to simplify the study. This term consisted of the laser used and their type of polarization. It is noticed that the variation of F_R in the long-term has undergone a strong fluctuation due in principle to variations in abundance. Which implies that the variation of centroid has no effect on the F_R's variations in a long-term. In this case, the centroid can be considered as a constant in equation 3. Return flux variations depends also to sites,

when the difference of 0.1 of T_{atmo} varies the F_R about 3 au (see figure 10). Sodium LGS makes it possible to sweep almost all the sky (from 0 ° to 60 °) and makes the astronomical observationof one's choice. But as shown in Figure 11, the F_R decreases by almost a factor of 4 au from zenith to the 60 ° angle.

5. Perspective

Our aim is to build global models where we can study all mesospheric sodium phenomena and their contributions in variation of LGS's parameters like F_R and LGS elongation. It is also hoped that these models can be applied on a long-term, annual or nocturnal basis, depending on the phenomena that dominate the mesospheric sodium layer on these periods.

References

[1] Moussaoui, N et al., 2010, "*Statistics of the sodium layer parameters at low geographic latitude and its impact on the adaptive–optics sodium laser guide star characteristics*", A&A, 511, A31.

[2] Djaidri, F., 2012, *"Effets des variations nocturnes des paramètres de la couche de sodium mésosphérique sur les caractéristiques des étoiles de référence (sodium LGSs)* ", USTHB, Alger, Thèse de Magister.- N° : 34/ 012-M/ PH.

[3] Moussaoui, N et al., 2009,*"Dependence of sodium laser guide star photon return on geomagnetic field"*, A&A, 501, 793–799.

[4] Bonaccini Calia, D., 2012, *"The ESO transportable LGS Unit for measurements of the LGS photon return and other experiments"*, Proc. SPIE 8450, Modern Technologies in Space- and Ground-based Telescopes and Instrumentation II, 84501R.

[5] https://www.google.fr/search?q=adaptive+optics&

[6] http://www.eso.org/public/announcements/ann14012/

[7] Hugot, E., 2007. *"Optique Astronomique et Élasticité"*, Thèse de doctorat/ Université de Provence-Aix-Marseille I.

[8] https://www.google.fr/search?q=220px+Comparison_optical_telescope_primary_mirrors.svg

[9] Simonich D. M et al., 1979, **"***The mesospheric sodium layer at 23° S: Nocturnal and seasonal variations***"**, Journal of Geophysical Research. - A4: Vol. 84. - pp. 1543-1550.

[10] Clemesha B. R. et al., 1997, *"Long-term and solar cycle changes in the atmospheric sodium layer"***,** Journal of Atmospheric and Solar-Terrestrial Physics. - No 13: Vol. 59. - pp. 1673-1678.